Asian Journal of Chemistry; Vol. 26, No. 11 (2014), 3129-3133

ASIAN JOURNAL OF CHEMISTRY

http://dx.doi.org/10.14233/ajchem.2014.15832

Preparation and Enhancement of Luminescent Intensity of New Rare Earth Molybdate $NaLa(MoO_4)_2:Eu^{3+}$ Phosphors

YONG-QING ZHAI*, JIAN MA, ZHI-CHUN HU, JIA-JIA ZHAO, MENG-YAO YANG and LEI ZHAO

College of Chemistry and Environmental Science, Hebei University, Baoding 071002, P.R. China

*Corresponding author: Fax: +86 312 5079525; E-mail: zhaiyongqinghbu@163.com

Received: 25 May 2013; *Accepted*: 22 July 2013; *Published online*: 25 May 2014; AJC-15198

Novel red-emitting rare earth molybdate phosphors $NaLa(MoO_4)_2:Eu^{3+}$ have been successfully synthesized by sol-gel method assisted by microwave. The as-synthesized samples were characterized by means of Fourier transform infrared spectroscopy, X-ray diffraction and Fluorescence spectrophotometer, respectively. The results show that the target product $NaLa(MoO_4)_2:Eu^{3+}$ have been synthesized by calcining precursor at 800 ºC. The obtained samples belong to tetragonal Scheelite-structure and $I4_1/a$ space group. The excitation spectrum of $NaLa(MoO_4)_2:Eu^{3+}$ has a broad band in the range of 250-350 nm and the main peak is at 301 nm. The broad band can be ascribed to the charge transfer band of Mo-O and Eu-O. The sharp lines in 350-500 nm range are due to 4*f*-4*f* transitions of Eu^{3+}. The emission spectrum contains a series of narrow peaks, with the main peak at 616 nm originated from the electric dipole transition of $^5D_0 \rightarrow {}^7F_2$ of Eu^{3+}. The appropriate doping amount of Bi^{3+} and flux NH_4F can enhance luminescent intensity of the sample effectively.

Keywords: $NaLa(MoO_4)_2:Eu^{3+}$, Sol-gel method assisted by microwave, Rare earth molybdate, Red-emitting phosphors.

INTRODUCTION

Recently, white light emitting diodes (LEDs) have been applied widely in many fields, such as auto lamp, LCD screen, the landscape lighting and other emerging areas[1-3]. They have attracted much attention due to their small size, high luminous reliability, long lifetime, low energy consumption and environment-friendly characteristics[4]. The most efficient method to obtain the white light is phosphor-converted. Nevertheless, the traditional red-emitting phosphor used for LED shows a rather low red emission under near-UV light excitation[5]. Therefore, it is indispensable to seek novel red phosphors that can be effectively excited by near-UV light.

Double molybdates $AB(MoO_4)_2$ (A = Li^+, Na^+, K^+, Rb^+, Cs^+; B = trivalent rare earth ions), with Scheelite-like structure, show high physical and chemical stability, strong water persistence. They are regarded as effective luminescent hosts[2]. In such double molybdates structure, the structural framework is composed of tetrahedral MoO_4^{2-}, the alkaline ions and rare earth ions are randomly distributed over the cation sites, the different cations with different radii in the host compound would arouse some change in the sub-lattice structure around the luminescent center ions and then result in different photoluminescent properties[6]. Therefore, $AB(MoO_4)_2$ double molybdate phosphors have recently received much attention. Mo *et al.*[7] synthesized a series of $NaGd(MO_4)_2:R$(M = W, Mo, R = Eu^{3+}, Sm^{3+}, Bi^{3+}) phosphors by solid state reaction at 900 ºC for 5 h. Sun *et al.*[8] synthesized shuttle-like $NaLa(MoO_4)_2:Eu^{3+}$ microcrystals under hydrothermal condition of 180 ºC for 16 h. The samples can solely be efficiently excited at 300 nm. However, solid state reaction requires higher temperature and longer reaction time and products have large particle size and irregular surface appearance. For hydrothermal method, although the morphology and size of the products can be well controlled, the reaction device is complicated and the reaction period is long.

In the present work, new red-emitting phosphors $NaLa(MoO_4)_2:Eu^{3+}$ were prepared by sol-gel method assisted by microwave. This method has a lot of advantages, such as simple operation, homogeneous composition, uniform particle size and the time for the gelling and drying can be remarkably shortened under the microwave radiation. It provides a new idea for saving energy and reducing energy consumption. The obtained samples exhibits excellent luminescent properties and can be excited effectively by UV at 301 nm, NUV at 395 nm and blue light at 464 nm. Hence, as-synthesized $NaLa(MoO_4)_2:Eu^{3+}$ shows good prospect for red phosphors of white LED. Moreover, the influences of co-doped Bi^{3+} concentration and fluxing agent NH_4F on the fluorescent properties of samples were also investigated.

EXPERIMENTAL

$(NH_4)_6Mo_7O_{24}·4H_2O$, HNO_3, $NaNO_3$, Eu_2O_3, La_2O_3, $Bi(NO_3)_3$, NH_4F, citric acid and aqueous ammonia were used as starting materials. They were all analytical reagents (AR).

$NaLa(MoO_4)_2:Eu^{3+}$ phosphor was synthesized by sol-gel method assisted by microwave. Firstly, Eu_2O_3 and La_2O_3 were dissolved, respectively in appropriate HNO_3 to prepare $Eu(NO_3)_3$ and $La(NO_3)_3$ solution, then the accurate concentrations were determined by EDTA complexing titration to ensure a desired stoichimetry. According to the stoichiometric ratio of target product, $NaNO_3$, $(NH_4)_6Mo_7O_{24}·4H_2O$, citric acid, $Eu(NO_3)_3$ solution, $La(NO_3)_3$ solution and appropriate amount of distilled water were added into a 100 ml ceramic crucible. Then, the mixture was stirred to make the materials dissolve completely. Subsequently, a small amount of aqueous ammonia was added to adjust the pH value of the solution to 2-3. Next, the resulting solution was treated by ultrasonic wave for 5 min to make raw materials mix uniformly. Then the mixture was put into a WG700SL2011-KG microwave oven and heated under the power of middle-high fire for 6.5 min to evaporate superfluous water fast and form a transparent gel. Then the gel was dried in a drying oven at 90 ºC. After drying, the dry white loose and porous sample (which was called the precursor) was obtained. Finally, the precursor was ground into fine particles and calcined in muffle furnace at 800 ºC for 3 h to obtain the goal product.

Characterization: Fourier transform infrared (FTIR) spectra were registered as KBr pellets by using a Nicolet 380 Fourier transform infrared spectrometer. Phase structure and crystallization of synthesized samples were characterized by X-ray diffraction analysis (XRD) with a Y2000 diffractometer using CuK_α radiation source (30 kV × 20 mA, λ = 0.154178 nm). The excitation and emission spectra of the samples were recorded on an F-380 fluorescence spectrophotometer. All measurements were performed at room temperature.

RESULTS AND DISCUSSION

FT-IR spectra analysis: The FT-IR spectra of the precursor and the sample obtained at 800 ºC for 3 h are shown in Fig. 1(a,b). In Fig. 1(a), the absorption bands near 3200 and 1616 cm^{-1} are assigned to -OH stretching vibration and H-O-H bending vibration of H_2O. The absorption peak around 1384 cm^{-1} is due to NO_3^- stretching vibration, which shows that trace of NO_3^- still exists in the precursor; The absorption peak near 1076 cm^{-1} can be ascribed to C-O stretching vibration; the absorption peak around 552 cm^{-1} is due to M-O stretching vibration in the citrate, which proves that metal ions have been formed the complex with citric acid in the precursor, meanwhile, the precursor contains a certain amount of water and organics.

From Fig. 1(b), it can be seen that the characteristic peaks of NO_3^- and C-O have disappeared after the precursor is calcined. The characteristic peaks of -OH are significantly reduced than before. The strong absorption peak near 805 cm^{-1} is due to Mo-O stretching vibration in MoO_4^{2-}. It can be seen that the precursor has been completely decomposed and transformed into molybdate after calcined at 800 ºC.

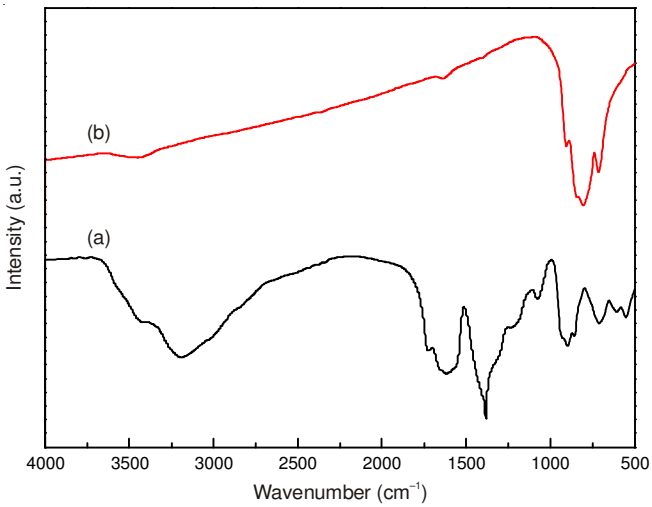

Fig. 1. IR spectra of the precursor (a) and the calcined sample (b)

X-Ray diffraction analysis of $NaLa(MoO_4)_2:Eu^{3+}$: Fig. 2 shows the X-ray diffraction pattern of as-synthesized $NaLa(MoO_4)_2:Eu^{3+}$ obtained by calcining the precursors at 800 ºC for 3 h. It can be seen that all of the peaks can be indexed to the $NaLa(MoO_4)_2$, which agrees well with the JCPDS card (No. 24-1103). According to that, the samples are pure tetragonal phase $NaLa(MoO_4)_2$ with space group $I4_1/a$.

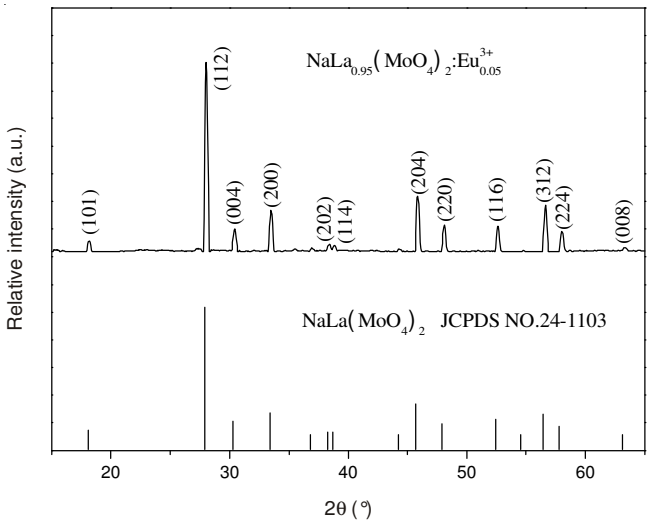

Fig. 2. XRD patterns of $NaLa(MoO_4)_2:Eu^{3+}$

In this pattern, the peaks of compounds of Eu can not be found, which indicates that Eu^{3+} has entered into the host lattice and have little effect on the crystal structure of the host $NaLa(MoO_4)_2$. The XRD peaks steadily shift toward the high angle side along with Eu^{3+} addition. This can be explained by the Bragg equation, λ = 2d sin θ (d is the distance between two crystalplanes, θ is the diffraction angle of an observed peak and λ is the X-ray wavelength). Since the radii of Eu^{3+} (0.106 nm) is smaller than that of La^{3+} (0.116 nm), when the La^{3+} ions in $NaLa(MoO_4)_2$ host lattice are substituted by Eu^{3+} ions, the crystal lattice constants as well as d-spacing decrease, hence, the diffraction angles shift to the higher angle side.

Excitation and emission spectrum of $NaLa(MoO_4)_2:Eu^{3+}$: The photoluminescence (PL) properties of the obtained

$NaLa(MoO_4)_2:Eu^{3+}$ samples were characterized by the photoluminescence excitation and emission spectra (Fig. 3). It can be seen that the excitation spectrum of $NaLa(MoO_4)_2:Eu^{3+}$ is composed of a broad band between 200 and 350 nm with a main peak at about 301 nm and some sharp peaks between 350 and 500 nm. The broad band can be ascribed to the charge transfer band (CTB) of Mo-O and Eu-O. The sharp peaks at 395 and 464 nm belong to the $^7F_0$-$^5L_6$ and $^7F_0$-$^5D_2$ transitions within the $4f^6$ configuration of Eu^{3+}, respectively. The CTB around 301 nm indicates that the energy transfer occurs from MoO_4^{2-} groups to the Eu^{3+} ions. It can also be seen that the intensity of CTB and peaks at 395 and 464 nm are all strong, which reveals that the energy transfer from MoO_4^{2-} to the Eu^{3+} is efficient[9].

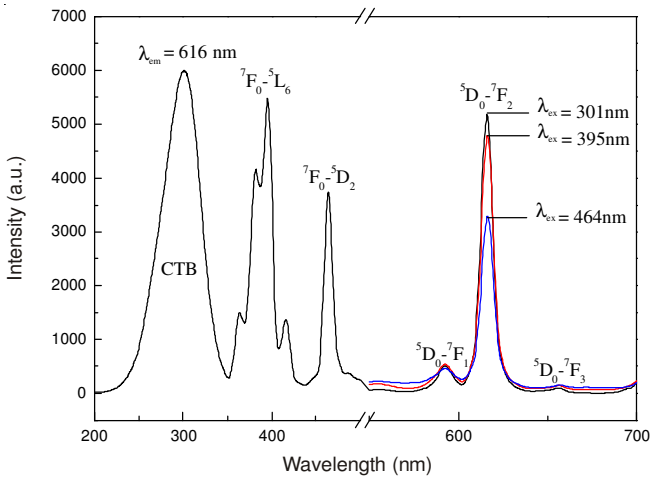

Fig. 3. Excitation and emission spectra of $NaLa(MoO_4)_2:Eu^{3+}$

Fig. 3 also shows the emission spectra of $NaLa(MoO_4)_2:Eu^{3+}$ sample excited by 301, 395 and 464 nm, respectively. It can be seen that all the emission spectra contain a group of lines at 592, 616 and 656 nm, which can be ascribed to $^5D_0$-^7F_J (J = 1, 2, 3) transition of the Eu^{3+} ions, respectively. According to the parity selection rule, when the Eu^{3+} ions are located at the site with an inversion symmetric center, the $^5D_0$-$^7F_1$ magnetic dipole transition is permitted, which results in orange-red emitting around 592 nm. While, if located at the site without an inversion symmetric center, as the opposite parity 5d configuration is mixed into $4f^n$ configuration, the parity selection rule is able to be lifted and f-f forbidden transition is partially released, the hypersensitive $^5D_0$-$^7F_2$ electric dipole transition will be permitted, which results in red emitting around 616 nm. For the samples $NaLa(MoO_4)_2:Eu^{3+}$ prepared in our experiment, the emission spectra are dominated by the $^5D_0$-$^7F_2$ (616 nm) transition of Eu^{3+}. It can be deduced that Eu^{3+} ions probably occupy non-inversion symmetric center in host lattice[10,11].

The excitation spectrum of the as-synthesized $NaLa(MoO_4)_2:Eu^{3+}$ phosphors covers a wide region between 200 and 500 nm and can be excited by UV at 301 nm, NUV at 395 nm and blue light at 464 nm effectively. So it can match well with UV-, NUV- and Blue-LED chip, displaying a great potential for practical applications.

Effect of co-doped Bi^{3+} ions on the structure and luminescent properties of $NaLa(MoO_4)_2:Eu^{3+}$: By changing the doping amount of Bi^{3+}, a series of phosphors $NaLa_{0.95-x}(MoO_4)_2:Eu^{3+}_{0.05},Bi_x$ (x = 0, 0.02, 0.05, 0.08, 0.10) were prepared successfully under the condition of constant Eu^{3+} concentration in the host lattice. The XRD patterns of the $NaLa_{0.95-x}(MoO_4)_2:Eu^{3+}_{0.05},Bi^{3+}_x$ (x = 0.02, 0.05, 0.08, 0.10) samples are shown in Fig. 4. It can be seen that all of the peaks can be indexed to the $NaLa(MoO_4)_2$, which agrees well with the JCPDS card (NO. 24-1103). The peaks of compounds of Bi can not be found, which indicates that doping small amount of Bi^{3+} has little effect on the crystal structure of the host $NaLa(MoO_4)_2$. The reason is that the radius of Bi^{3+} (0.117 nm) is similar to that of La^{3+} (0.116 nm).

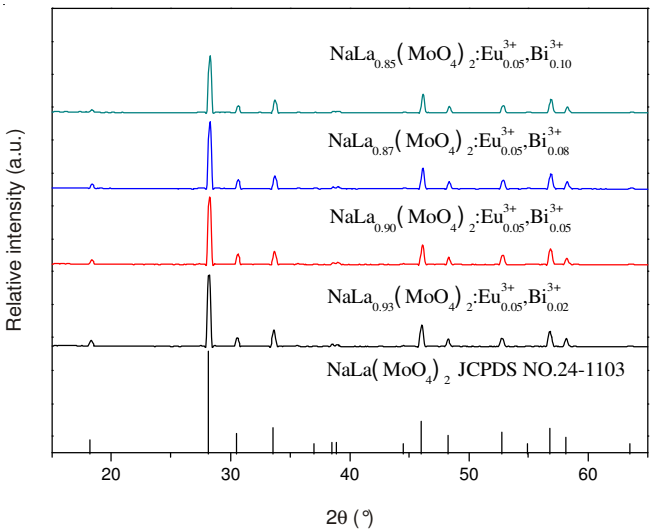

Fig. 4. XRD patterns of $NaLa_{0.95-x}(MoO_4)_2:Eu^{3+}_{0.05},Bi^{3+}_x$ (x = 0.02, 0.05, 0.08, 0.10)

The excitation spectra of the samples are shown in Fig. 5. It can be seen that the CTB of Mo-O and Eu-O is widened and the main excitation peak shifts from 301-324 nm for the doping of Bi^{3+}. That would be mainly due to the CTB of Bi-O and the self-absorption of Bi^{3+} from ground state $^1S_0$ to the excited state $^3P_1$[12].

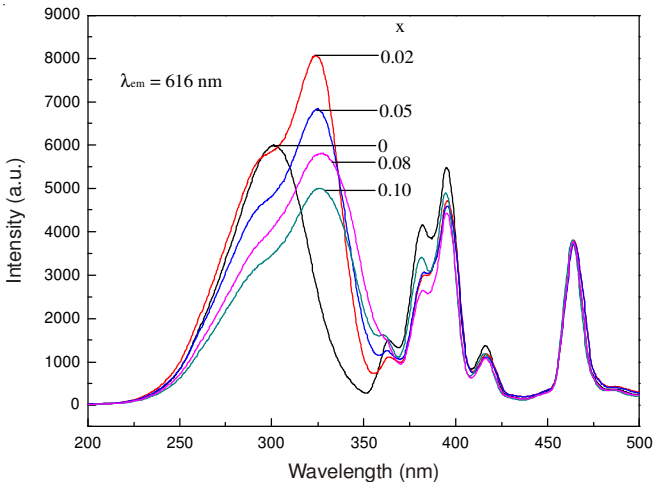

Fig. 5. Excitation spectra of $NaLa_{0.95-x}(MoO_4)_2:Eu^{3+}_{0.05},Bi^{3+}_x$

The emission spectra of the samples $NaLa_{0.95-x}(MoO_4)_2:Eu^{3+}_{0.05},Bi^{3+}_x$ are shown in Fig. 6. It can be seen that the Bi^{3+} concentration (x) has little effect on the shape and position of

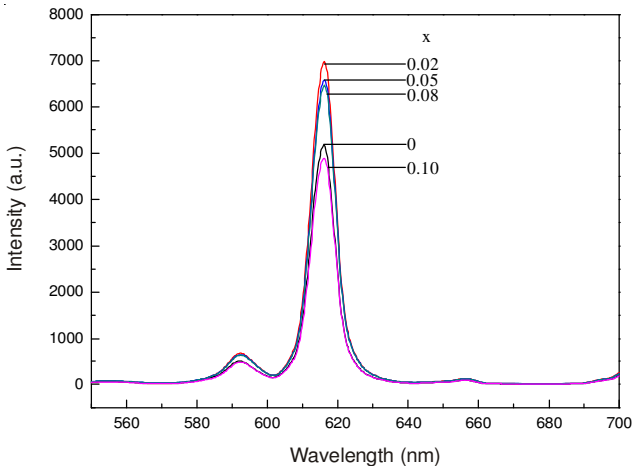

Fig. 6. Emission spectra of $NaLa_{0.95-x}(MoO_4)_2:Eu^{3+}_{0.05},Bi^{3+}_x$

emission peaks, but has great effect on the intensity. When Bi^{3+} doping concentration x < 0.02, the emission intensity at 616 nm increases with the increase of x; the emission intensity is up to the strongest when x = 0.02, compared with un-doped sample, the intensity is increased 40 %; if x > 0.02, the emission intensity begins to decrease. The reason is that, at very low concentration, the sensitization from Bi^{3+} to Eu^{3+} increases with Bi^{3+} concentration. Exceeding the optimum concentration, the energy transfer between Bi^{3+} ions become less efficient; therefore, higher Bi^{3+} doping concentration dissipate the absorbed energy non-radiatively instead of transferring the absorbed energy from Bi^{3+} to Eu^{3+}, resulting in less energy transfer from Bi^{3+} to Eu^{3+} [13]. Moreover, doping of superfluous Bi^{3+} ions may cause oversize distortion in the lattice, which also leads to fluorescence quenching. Thus, the optimum concentration of Bi^{3+} x = 0.02.

Effect of fluxing agent on the structure and luminescent properties of $NaLa(MoO_4)_2:Eu^{3+}$: Diffusion is one of the significant processes affecting the rate of solid reaction. Usually, proper fluxing agent is added into the system to decrease melting point and improve the diffusion rate. For luminescent materials, it is beneficial to the formation of the matrix, the doped ions entering into matrix lattice easily and improving luminescence intensity of products. In our experiment, NH_4F was used as fluxing agent and the effect of NH_4F dosage (y, *i.e.*, the mass fraction of NH_4F to sample) on the structure and luminescent properties of $NaLa(MoO_4)_2:Eu^{3+}$ was investigated.

Fig. 7 shows the XRD patterns of as-synthesized $NaLa(MoO_4)_2:Eu^{3+}$ samples under different dosage of NH_4F. It can be seen that all the diffraction peaks of four samples can agree well with tetragonal Scheelite-type $NaLa(MoO_4)_2$, no additional peaks of other phases can be detected, which indicates that doping small amount of NH_4F has little effect on the crystal structure of host $NaLa(MoO_4)_2$. In addition, the diffraction peaks of the samples with NH_4F are sharp and stronger than that of the sample without NH_4F, revealing that the products have higher crystallinity.

Fig. 8 shows the excitation spectra of the samples. It can be known that the dosage of NH_4F has little effect on the shape and position of excitation peaks, merely has some effect on the intensity.

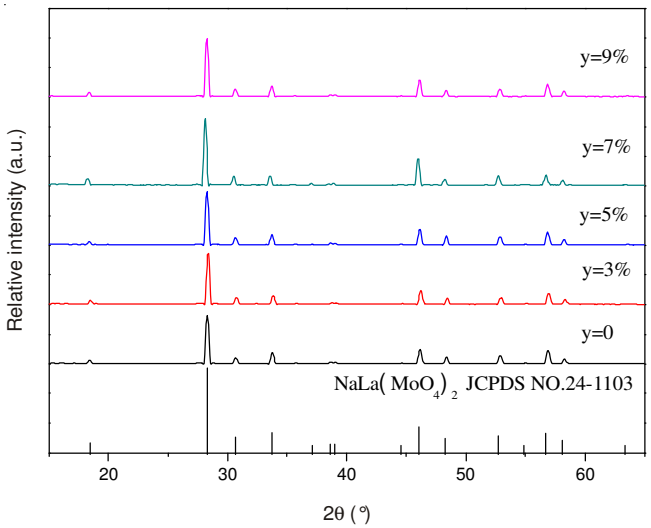

Fig. 7. XRD patterns of $NaLa(MoO_4)_2:Eu^{3+}$ under different dosage(y) of NH_4F

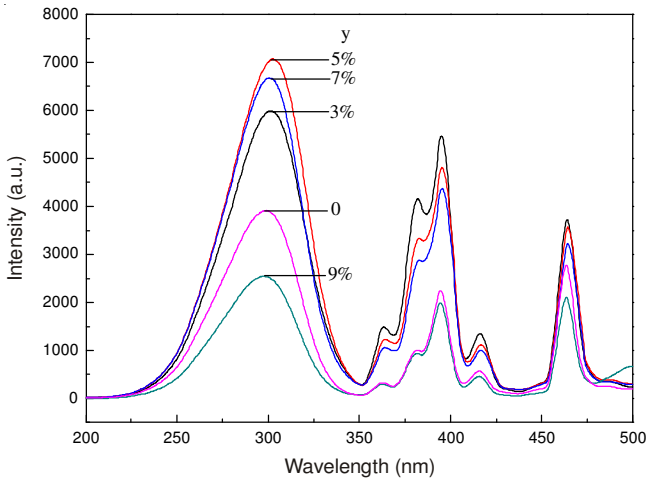

Fig. 8. Excitation spectra of $NaLa(MoO_4)_2:Eu^{3+}$ under different dosage(y) of NH_4F

The emission spectra of the samples are shown in Fig. 9. It can be seen that the dosage of NH_4F has little effect on the shape and position of emission peaks, but has great effect on the intensity. The emission intensity at 616 nm increases with increasing y value from 0-5 %. The emission intensity with y = 5 % is the strongest. Compared with the sample without fluxing agent, the intensity is enhanced 40 %. It is known that the ionic radius of F^- (131 pm) is similar to that of O^{2-} (135 pm) and the substitution amount of F^- for O^{2-} is not much. When the O^{2-} ions are partially replaced by the F^- ions, the symmetry of the Eu^{3+} connected with F^- was reduced from S_4 to C_1 [14]. This reduction is favourable to $^5D_0$-$^7F_2$ dipole transition of Eu^{3+} and makes the emission intensity of $^5D_0$-$^7F_2$ transition increase. Meanwhile, F^- doping reduces the phonon energy, which remarkably enhances the probability of $^5D_0$-$^7F_2$ transition and the luminescent intensity.

As shown in Fig. 9 the emission intensity starts to decrease when y value exceeds 5 %. The reason may be that excessive NH_4F destroys the crystal structure of the host to some extent, which makes the luminescence efficiency of Eu^{3+} decrease. Therefore, the suitable y(NH_4F) is 5 %.

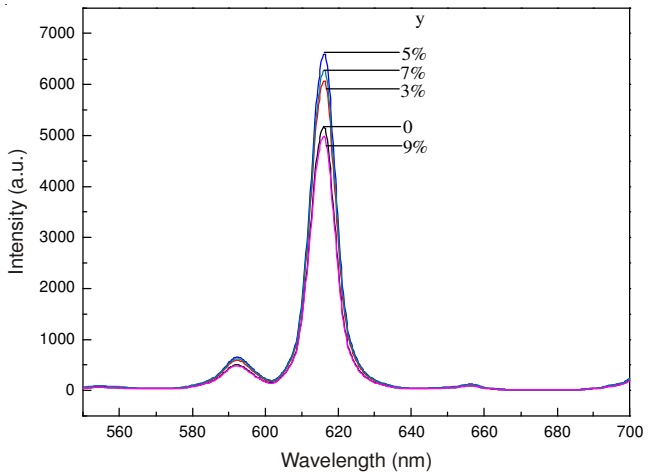

Fig. 9. Emission spectra of $NaLa(MoO_4)_2:Eu^{3+}$ under different dosage(y) of NH_4F

Conclusion

Novel red-emitting phosphors $NaLa(MoO_4)_2:Eu^{3+}$ were prepared by sol-gel method assisted by microwave. $NaLa(MoO_4)_2:Eu^{3+}$ phosphors belong to a tetragonal Scheelite-structure with space group $I4_1/a$. The doping of Eu^{3+} has little effect on the host $NaLa(MoO_4)_2$. The excitation spectrum extends from 200-500 nm, which can be coupled well with the emission of UV- , NUV- and Blue-LED Chip. The emission spectrum mainly consists of a strong emission peak at 616 nm, so the samples present pure red-emitting. The luminescent intensity of $NaLa(MoO_4)_2:Eu^{3+}$ can be enhanced effectively by doping proper amount of Bi^{3+} or NH_4F. The optimum concentration of Bi^{3+} is 0.02 and the suitable dosage of NH_4F is 5 %.

ACKNOWLEDGEMENTS

This study was supported by National Natural Science Foundation of China (No. 50672020).

REFERENCES

1. X.H. He, J. Zhou, N. Lian, J.H. Sun and M.Y. Guan, *J. Lumin.*, **130**, 743 (2010).
2. Z.L. Wang, H.B. Liang, M.L. Gong and Q. Su, *J. Alloys Comp.*, **432**, 308 (2007).
3. H. Md, H.L. Lee and D.K. Kim, *J. Alloys Compd.*, **481**, 792 (2009).
4. Y.Q. Zhai, Z.J. You, Y.H. Liu, Y.P. Sun and Q.Q. Ji, *J. Rare Earth*, **30**, 114 (2012).
5. Y.Z. Li, S.W. Jian, R.W. Jing, Z.J. Fu, H.Y. Ling and L.H. Jun, *J. Alloys Comp.*, **476**, 390 (2009).
6. X.H. He, M.Y. Guan, Z.C. Li, T.M. Shang, N. Lian and Q.F. Zou, *J. Rare Earth*, **28**, 878 (2010).
7. F.W. Mo, L.Y. Zhou, P. Qi, Z.G. Fu and J.L. Zhi, *Ceram. Int.*, **38**, 6289 (2012).
8. J.Y. Sun, C. Cao and H.Y. Du, *Acta Phys. Sin*, **60**, 127801 (2011).
9. G. Jia, S.W. Ding, C.M. Huang, L.F. Li, C.Z. Wang, X.B. Song, L. Song and Z.L. *Microspheres Opt. Mater.*, **35**, 288 (2012).
10. G. Blasse, *Chem. Phys. Lett.*, **20**, 573 (1973).
11. L.D. Sun, C. Qian, C.S. Liao, X.L. Wang and C.H. Yan, *Solid State Commum.*, **119**, 393 (2001).
12. B. Yan and J.H. Wu, *Mater. Chem. Phys.*, **116**, 67 (2009).
13. S.X. Yan, J.H. Zhuang, S.Z. Lu, X.G. Ren, Z.J. Nie and X.J. Wang, *J. Phys. Chem. C*, **111**, 13256 (2007).
14. J.G. Wang, X.P. Jing, C.H. Yan, J.H. Lin and F.H. Liao, *J. Lumin.*, **121**, 59 (2006).